5th International Conference on Biaxial/Multiaxial Fatigue and Fracture Cracow'97, Poland

Giora SHATIL* and John TWIDELL**

Fatigue Performance Study of the 60m Diameter Steel Rotor Spar of the LS1 3MW Wind Turbine Generator

* Lecturer, Faculty of Engineering, University of the West of England, Frenchay Campus, Coldharbour Lane, Bristol, UK.

** Professor and Director, The AMSET Center, Queens Building, De Montfort University, Leicester, UK.

Keywords: Fatigue life, Wind Generator, Strain data, Steel rotor, Miner's rule

ABSTRACT: Strain data has been acquired in the form of continuous rainflow cycles and periodic 'snap-shots' from various locations along the steel spar of the LS1 wind turbine rotor. Estimates of the rotor fatigue performance were obtained using; (a) S-N approach to estimate crack initiation life, employing Miner's rule for summation of damage; and, (b) Damage tolerance analysis for propagation of cracks to final failure using fracture mechanics. The analysis indicated that life of the structure with initial defects could be shorter by a factor of 3-4 on the lives obtained using the S-N approach. However, the fracture mechanics estimation of the crack propagation rate was dependent on the assumed initial conditions such as initial defect size, mean stress (R-ratio) and treshold values. Similar lives to crack initiation were estimated from using on-line continuous data and from using extrapolation of short period reference sets of data. The annual fatigue damage was estimated using long term wind measurements and wind turbine operation modes.

Introduction

Inadequate fatigue design of wind turbine generators has been reported in the past to be responsible to a premature structural failure in many cases (1,2). This was predominately due to the complex loading experiences by the wind turbine structures during their lifetime,

but it was also due to the designer's emphasis on aerodynamic efficiency and cost savings in order to make the generation of electricity from the wind economic. The fatigue cycles in a rotor of a typical horizontal axes wind turbine are dominated by the stochastic, or random, nature of the wind that prevail in the site, combined with additional deterministic component that is dependent of the rotor weight and rotation and of the operating conditions (3). A commercial modern wind generator has a life expectancy of 20 to 30 years and the rotor structure has to survive approximately 10^8 fatigue cycles from both, rotor rotation and wind fluctuations. A survey of this subject, and an extensive description of wind generators fatigue has been previously given by Stherland et al (2).

Published research in the area of fatigue of wind turbines was found to be limited. The models that were used to estimate the life of the structures appeared to concentrate in two areas: (a) The applications of the traditional S-N curve, using the Miner's summation rule with some assumptions with regard to long term damage accumulation (2) and, (b) a theoretical solutions for the estimation of cycle ranges distribution using power spectral density analysis (4,5). A fatigue crack propagation approach have also being used in earlier work to estimate the life of a large rotor (6,7).

The LS1, 3MW rated power, horizontal axes wind generator in Orkney, Scotland, Fig. 1, has the largest wind generation capacity in Europe. It is one of the few multi-megawatt machines that were designed in the early eighties. The machine is two bladed tip-controlled with 60m diameter steel rotor and it was designed, constructed and commissioned in 1988 by the Wind Energy Group (8,9,10). The LS1 has so far generated over 10 GWh from over seven thousand hours of rotations. It is now operated and maintained on lease from the DTI by Orkney Sustainable Energy Ltd, having been recomission by the AMSET Centre of De Montfort University, Leicester (11).

The following investigation has used results from the extensive fatigue monitoring programme of the LS1 rotor that was carried out between 1988 and 1990 (10). During that time an 'on-line' monitoring facility accumulated 'rainflow' counted strain cycles whenever the wind turbine was operational. In addition, reference (or campaign) data at short snap-shots of 10 minutes were acquired, which were also suitable for fatigue analysis. Estimates of fatigue life were obtained using three methods; (a) the 'rainflow' counted strain cycles (12) and an S-N curve with Miner's rule damage summation, (b) repeats of the reference 'snap-shots' data and the S-N curve with Miner's rule damage summation and, (c) a fracture

mechanics approach to analyse repeats of the reference data. The procedures used for the three methods are shown in Fig. 3.

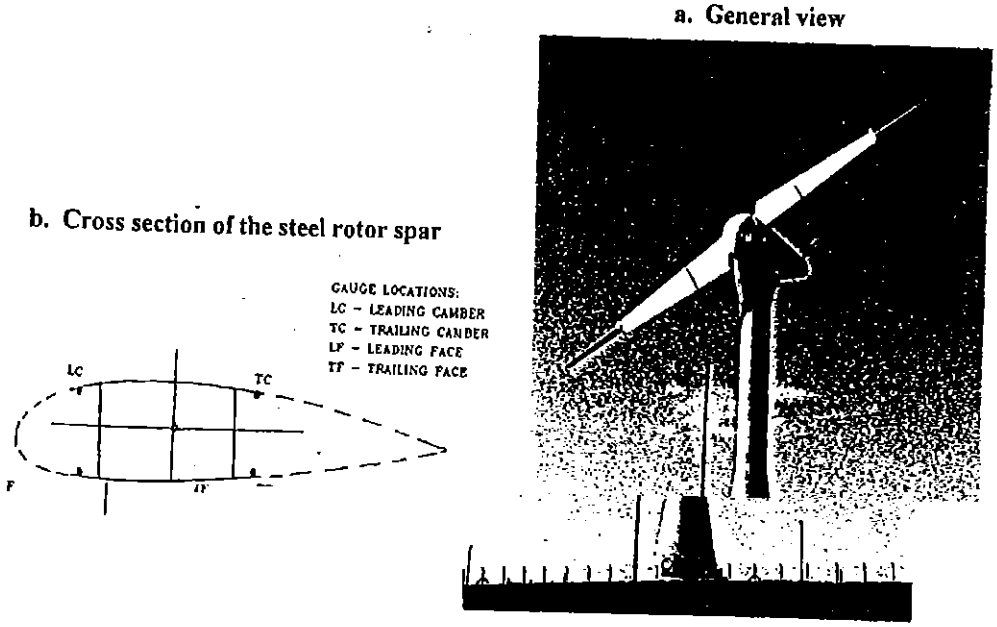

Fig.1 The LS1 wind generator in Orkney, Scotland

Material, structure and data availability

The LS1 rotor main spar has a welded structure that was built with EN50D (BS4360) structural steel (0.2-0.4% carbon %/weight, and approximately 355 MPa and 480 MPa Yield and ultimate stresses, respectively). "1/4 bridge" strain gauges were installed at different radii near the rotor spar joints. At each of these joints at least four gauges were located as follows: leading face (LF), leading camber (LC), trailing face (TF) and trailing camber (TC), Fig. 1. These joints were subjected to both, in-plane and out-of-plane bending moments.

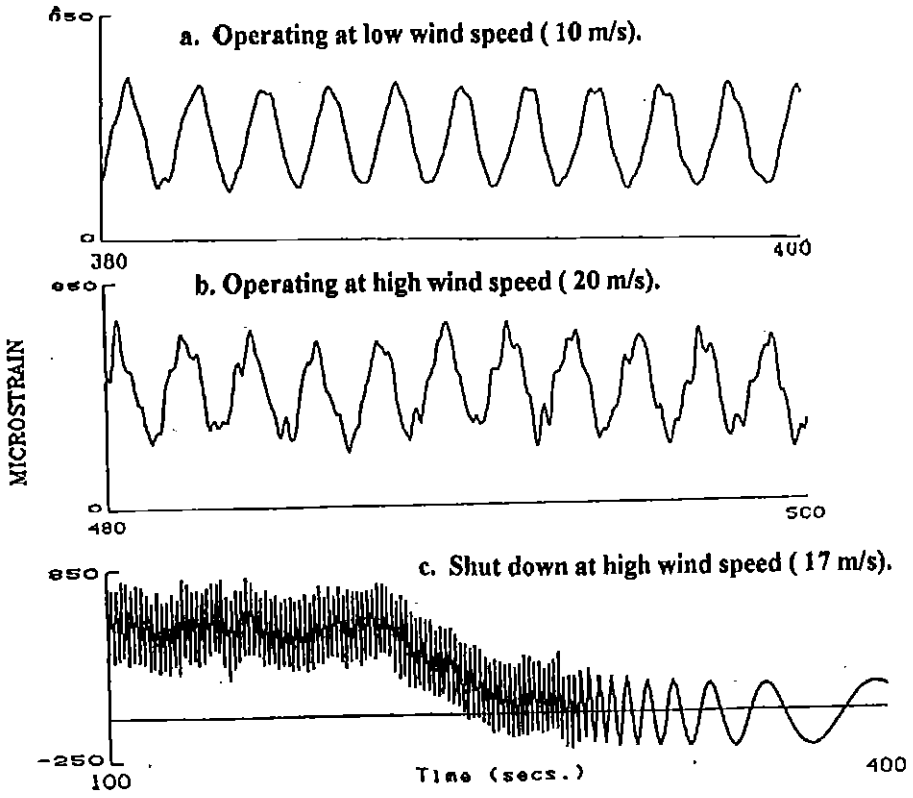

Fig.1 Examples of strain time histories measured on the rotor at 9m radius, TF location

The measured on-line rainflow count was collected in strain bins of cycles range and mean strains. Cycles were sorted and stored in a matrix of 64X64 bins of mean strain and strain range. The accumulative cycles in each of these bins were further subdivided into ten different Modes of the wind turbine operation as follows. Modes 1 and 2 for start up in low and high winds. Modes 3 to 8 were used for increasing winds between 0 to 34 m/s for data collected while the generator was operational. Modes 9 and 10 were used for stationary conditions at high and low winds. The time covered by each mode of operation was recorded daily. Similar modes of operation were also used as a basis to trigger the ten minutes "snap-shots" data. Approximately ten "snap-shots" time histories were collected at each Mode of operation.

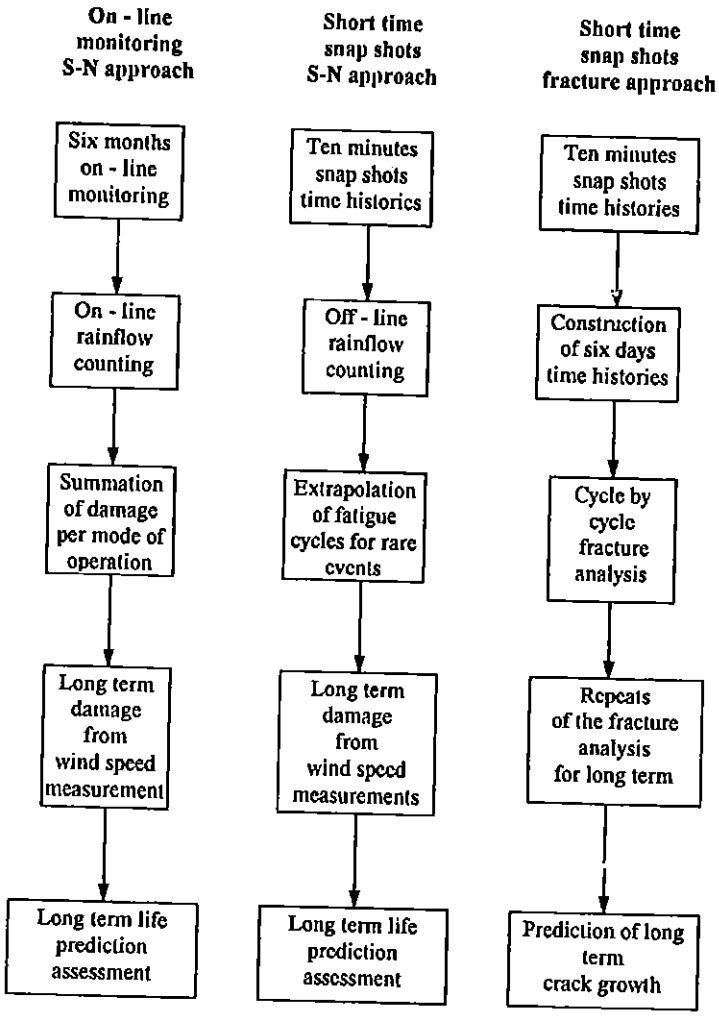

Fig.3 Life assessment procedures used for the LS1 wind generator rotor spar

Due to the weight of the LS1 rotor (over 30 tonnes) the dominant factor defining the strain range for the LS1 rotor spar is the once per revolution gravity cycle (1P). At wind speed below about 12 m/s, the strain fluctuations are very nearly sinusoidal, Fig. 2a. However, at higher wind speeds a higher frequency components are introduced on top of the one per revolution cycles, Fig. 2b. These is caused by short term fluctuations due to short gusts. Such high frequency components enhance the dominant gravity cycles. However, the largest ranges of strain cycles were obtained from start/stop operations of the generator,

Fig. 2c. These cycles exhibited a change in the mean strain, introducing a cycle range that is 2-3 times larger as compared with a typical operational cycle range. Histograms of rainflow counted cycles as a function of mean strain and strain range are given in Fig. 4 for four locations along the rotor spar. The bins having the largest number of cycles are related to the dominant gravity, one per revolution cycles , Fig. 4.

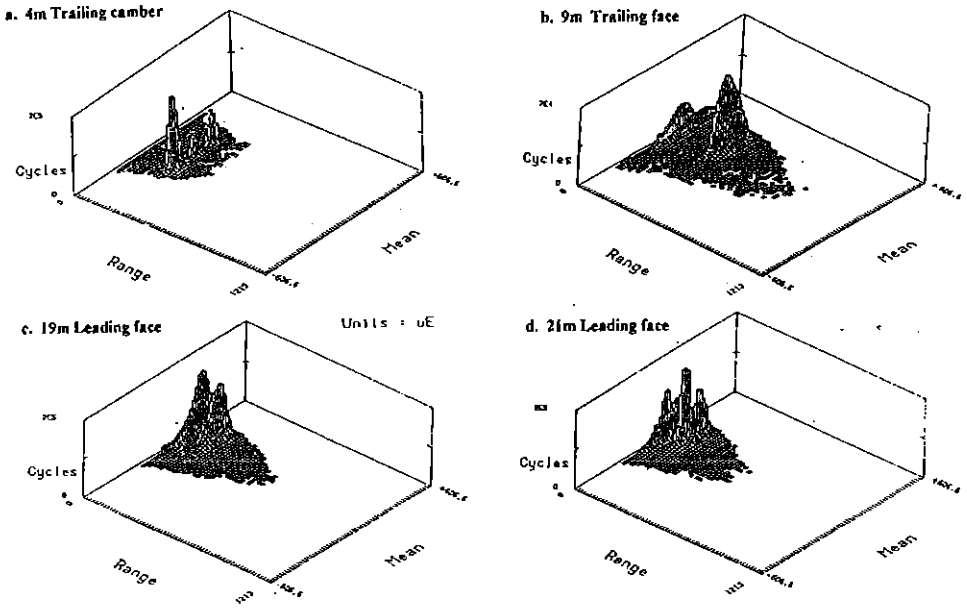

Fig.4 Cycles histograms as a function of mean strain and strain range as measured at four radii along the rotor spar

Estimated life using the on-line data

The fatigue investigation of the on-line data was carried out by employing an S-N curve that was derived from analysis of experimental results using large welded specimens. These specimens were manufactured similarly to the rotor spar welded joints and tested to failure under constant amplitude stress range (13). However, the experimental S-N curve was modified, using the BS5400 (14) approach to random fatigue. The S-N curve slope was increased by 2 for stress ranges with over 10^7 cycles to failure as follows:

$$N\Delta\sigma^{m} = K \tag{1}$$

$m = 10.8$ and $K = 2.0 \times 10^{29}$ for $\Delta\sigma \geq 116$ MPa $(N \leq 10^7$ cycles)

$m = 12.8$ and $K = 2.7 \times 10^{33}$ for $\Delta\sigma > 116$ MPa $(N > 10^7$ cycles)

Where $\Delta\sigma$ is expressed in MPa and N_f is the experimental number of cycles to failure. N is the experimentally obtained number of cycles to failure at a specific constant amplitude stress range level. The structural stress range, $\Delta\sigma$, was considered to be dominated by the maximum principal stress, in a direction along the spar length and was calculated from the strain gauges using Young Modulus of 2 GPa.

Cumulative fatigue damage (D_i) was estimated from cycles obtained at each stress bin ($\Delta\sigma$) and was calculated according to Miner's rule employing equation 1 as follows :

$$\frac{n_i}{N_i} = \frac{n_i \Delta\sigma}{K} = D_i \tag{2}$$

Where n_i is the number of cycles monitored at a singular bin of stress range and N_i is the correspondent experimental number of cycles to failure in the S-N curve from equation 1. Linear summation of the damage from all the stress range bins was carried out as follows:

$$\sum_{i=1}^{64} \frac{n_i}{N_i} = D \tag{3}$$

It was assumed that fatigue failure occurred when D is equal to 1.

Initially, fatigue analysis was carried out using the monitored data without making any long term assumptions. This gave an indication of the variation of fatigue damage with spar location, wind speed and operating conditions.

This initial fatigue analysis indicated four spar locations with higher damage accumulation rate then other locations, e.g. at 4, 9, 19 and 21 meters of the rotor radii. Cycles and Damage histograms for these four locations are shown in Fig. 4 and Fig. 5, respectively. The damage at the 4m radius is dominated by the once per revolution gravity cycles. At the 9m location a significant proportion of the damage is developed at the highest stress cycles. For the 19m and 21m the damage is almost entirely developed by a small number of high stress cycles.

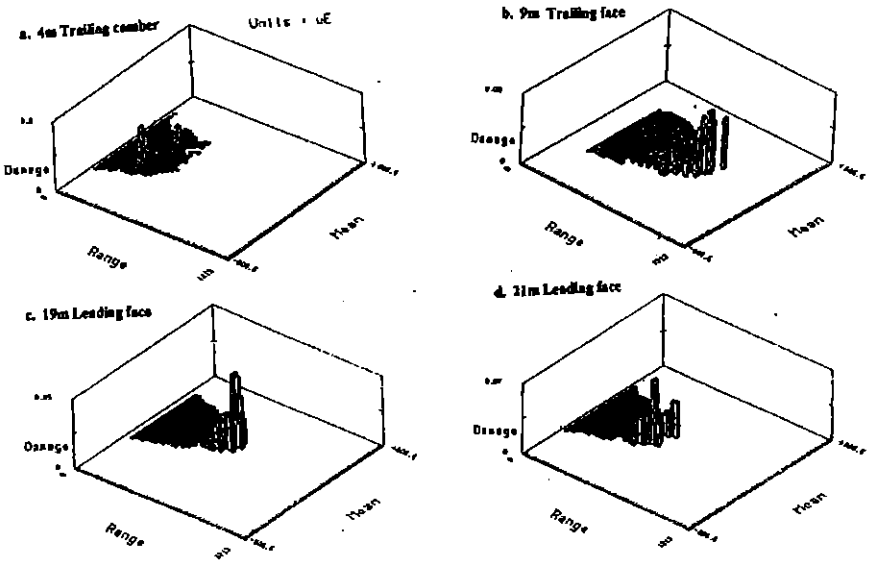

Fig.4 Fatigue damage as a function of mean strain and strain range as measured at four radii along the rotor spar

The long term estimate of the fatigue damage was carried out by assuming that all likely events have occurred during the monitoring period, but not necessarily in the proportion anticipated over one year of operation. Therefore, a breakdown of the assumed long term distribution of the annual wind speed in the site, based on Burgar Hill Weibull distribution (10), identified the duration of each mode of operation during one year. The proportion of each mode of operation over one year that was obtained from the wind data and was used to modify the initial damage summations as follows:

$$D_{\text{damage per year}} = \sum_{\text{Mode 1}}^{\text{Mode n}} \left\{ \frac{D_{Mi}}{D_{Ti}} \frac{t_{mi}}{t_{\text{annual}}} \right\} \qquad (4)$$

Where : D_{Mi} = monitored data fatigue damage per mode i (using Miner's rule summation, equations 2 and 3)

D_T = Total monitored data fatigue damage

t_{mi} = Estimated duration for mode i

t_{annual} = Annual number of hours of operation

The life of the structure, in years, was the reciprocal of the calculated damage in equation 4. A comparison between the predicted damage per mode and the expected duration as a percentage of a total in one year is shown in Fig. 6 for four radii along the rotor. In general, the damage accumulation rate is consistent with the most commonly prevailing wind in the site of between 10-16 m/s, irrespective of the measured location on the rotor. This mode was typically responsible for 34% of the total damage which is also approximately the proportion of the wind duration at that mode. However, Fig. 6 also indicates that as wind speed increases, the damage accumulation rate also increases, in particularly at outer radii where gravity loading is less dominant.

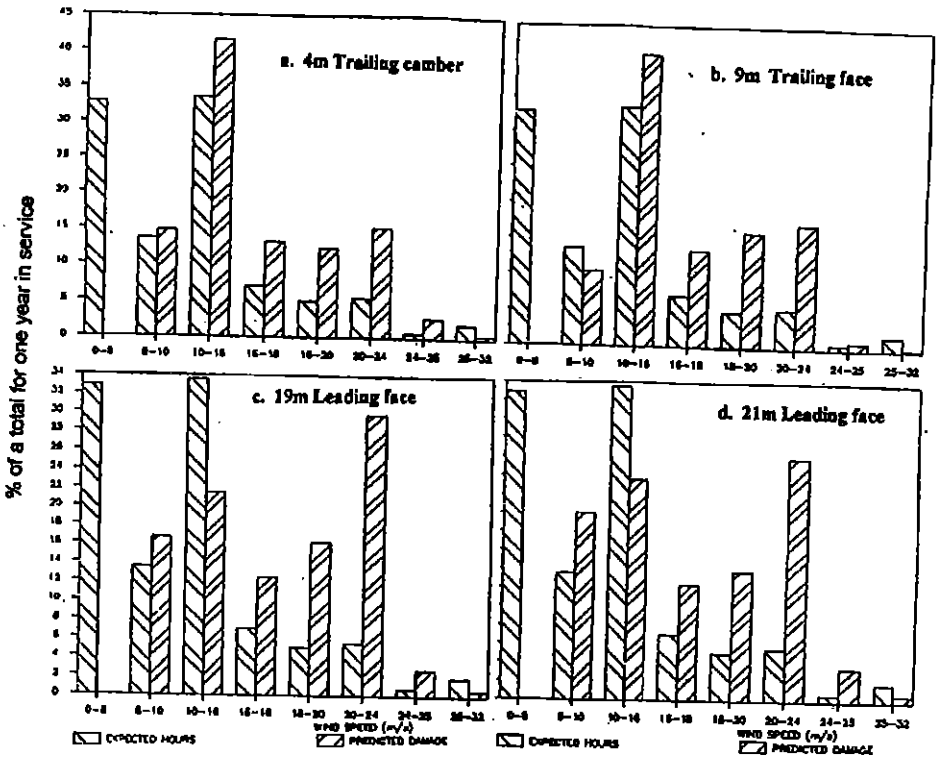

Fig.6 Comparison between the annual duration and predicted damage (as % of one year in service) for each mode of operation and at four spar radii

Estimated Life Reference Data

An alternative procedure for the life assessment was involved with the analysis of a relatively small quantity of time history data. A series of 10 minute sequences of rotor strain data were selected. These covered the full range of operational wind speeds and a selection of stop/start events. The damage accumulated from rainflow counts of each time-history series was then weighted and added to the total damage in a similar manner to the previous on-line analysis. An advantage of this analysis over the on-line analysis is that the effect of individual events, such as start/stop operations can be determined more precisely. However, the main disadvantage of this approach is that rare events are unlikely to be included, and therefore a statistical extrapolation is required.

Nine sets of data, that covered the full operational conditions and three shut down events at low, medium and high wind speeds were selected for the fatigue analysis at one location in the rotor that have shown the highest damage accumulation using the on-line data (9m TF). The proportion of the expected long term operational time that was allocated to each set and rainflow cycle counts was carried out similarly to the on-line data, employing a statistical extrapolation of the number of cycles for the rare events that might occur at higher stress bins. Fatigue damage estimation, identical to that carried out with the on-line data, was conducted using the reference data.

Estimated Life Using Fracture Mechanics

Using fracture mechanics method, the existence of a crack or defect was assumed and, through reference to material data, the crack growth was estimated. Therefore, the uncertainties due to (a) adopting the Miner's rule summation and (b) the inability to account for the sequence of cycles are removed. However, other factors such as the assumed initial crack size, threshold values and the existence of residual stresses had a major influence on the rate of crack growth to failure.

The analysis of crack growth was carried out using Paris law for fatigue crack growth, equation 5:

$$\frac{da}{dN} = C(\Delta K)^m \quad (5)$$

Where $\frac{da}{dN}$ (m/cycles) is the cyclic crack growth, ΔK (MPa$\sqrt{m}$) is the range of the stress intensity factor ($K_{maximum}$ - $K_{minimum}$) and m and C are material constants (15).

For the random fatigue the crack propagation rate was summed up by using a cycle by cycle analysis:

$$a_{final} = a_{initial} + \sum_{i=1}^{N}\left(\frac{da_i}{dN_i}\right) \quad (6)$$

Where a_{final} is the final crack length, $a_{initial}$ is the assumed initial defect and $\frac{da_i}{dN_i}$ is the rate of crack propagation of cycle i.

The fracture analysis was performed using the nCode KRAKEN commercial code. A Paris law coefficient (C) of 4.02×10^{-12} m/cycles and an exponent (m) of 3.6 were employed throughout the analysis. Two ΔK_{th} - R-ratio curves were used employing a linear relationships as follows:

$$(\Delta K_{th})_1 = 5.2 \text{ MPa}\sqrt{m} \quad \text{for R-ratio} = 0 \quad (7)$$
$$(\Delta K_{th})_2 = 2.0 \text{ MPa}\sqrt{m} \quad \text{for R-ratio} = 1$$

$$(\Delta K_{th})_1 = 6.7 \text{ MPa}\sqrt{m} \quad \text{for R-ratio} = 0 \quad (8)$$
$$(\Delta K_{th})_2 = 2.5 \text{ MPa}\sqrt{m} \quad \text{for R-ratio} = 1$$

Where R-ratio is the ratio between the minimum and maximum stresses of a cycle for a given crack size. Equation 7 was obtained using nCode lower bound database (16), while equation 8 have used values obtained from ESDU (17) lower bound. Two allowable initial defects of 1mm and 0.8mm long were examined in accordance with the rotor NDT inspection requirements (13). The aspect ratio between the thickness crack to the surface crack was taken as 0.5 throughout the analysis.

Data for the crack growth analysis were created by repetition of the 10 minute reference sets over 6 days. The sequence was initially constructed by following, as closely as possible, operating conditions that actually monitored during three, 24 hour, specific

wind periods. These three sets represented high, medium and low wind conditions. A six day continuos operation sequence was then developed using the three 24 hour sets and including start and stop events. Repetition of the six days sequence, together with an assumed non-operational period, resulted in a long term data set that was typical of the actual conditions experienced by the rotor.

A cycle by cycle fracture analysis was carried out for the 9m trailing face location on the rotor spar, assuming a range of initial conditions, material properties and loading definitions. The time to failure of the structure was assumed to be associated with a crack growth to a length of 7mm. This crack length was sufficient to define failure since typically, 95% of the simulated time to failure was spent during crack growth of less then 3mm, Fig. 7, and, thereafter, a fast propagation took place.

Results and Discussion

The long term fatigue life estimates are summarised in Table 1 for one spar joint at the 9m Trailing Face. These results assumed 20% increase in the measured stress spectrum. Table 1 shows that lives obtained from using the S-N method and employing on-line rainflow counting or reference data, exceeded the design life of 25 years by factor of 2 at least. Safe life was also predicted using initial defect of 1mm and assuming residual stress of 75 MPa and using equation 7 for the definition of the treshold values for crack propagation. These criteria approximately followed the rotor design specifications (13).

Of the three initial assumptions that were used in the fracture analysis the choice of ΔK_{th} - stress ratio curve has appeared to have the greatest influence on the estimated life. The threshold values obtained from nCode (16, equation 7) were considerably lower then those obtained from ESDU (17, equation 8) Consequently, a faster crack propagation rate and shorter life was obtained using the nCode curve, Table 1. The estimated rotor life was also highly dependent on the assumed initial defect size. For example a relatively small decrease of 0.2mm in the assumed initial defect, has resulted with factor of 3 on the predicted fatigue lives, Table 1.

The traditional S-N approach to fatigue damage is usually associated with the

concept of fatigue endurance limit, typically at around 10^7 cycles for fatigue at constant stress range and for structural steel (15). However, the number of random cycles that a typical wind turbine rotor experiences during a life time is extremely high, about 10^8 cycles, of which a high proportion are relatively small. Therefore, the assumption concerning the amount of damage from these small cycles can have a dramatic effect on the estimated life. Moreover, the fatigue investigation of the LS1 rotor has revealed that the life estimate is influenced by other factors that have not been included. For example, the assumed certainty of survival, the effect of the mean stress and an assumption with regard to a local stress concentration factors as well as changes in operation strategy and the site ambient conditions.

Table 1. Predicted Life of the LS1 Spar Rotor Using the Highest Stressed Location at the 9m Radius Trailing Face and Employing Stress Concentration Factor Of 1.2.

Analysis Type	Initial Defect Size mm	Residual Stress MPa	Predicted Lives in Years
SN curve and on-line rainflow counts	None	None	64
SN curve and Reference data	None	None	58
FM and Reference data with equation 8	1	75	Beyond 40 years
FM and Reference data with equation 7	1	75	12
FM and Reference data with equation 7	0.8	75	30
FM and Reference data with equation 7	1	50	30

Finally, Fig. 8 expresses the ratio between the proportion of damage per mode of operation to the proportion of the wind at that mode as damage intensity, for five locations along the rotor radius. Below the rated wind speed of 10 m/s the damage intensity is close to unity, whereas in high winds and at close to the rotor tip the intensity of damage

approaches 6. Fig. 8 demonstrate the dependence of the fatigue damage accumulation rate on mean wind speed, which therefore includes any affect of variation in ambient conditions and or changes of LS1 control features.

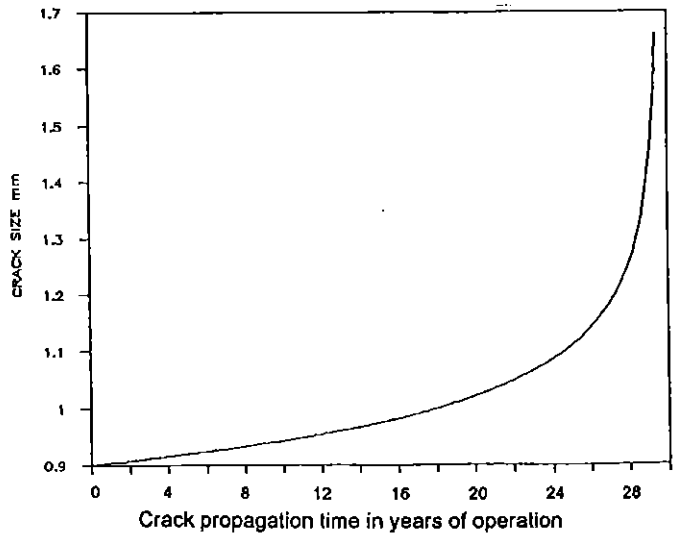

Fig. 7 Predicted crack growth from data measured at 9m radius, leading face of the rotor spar

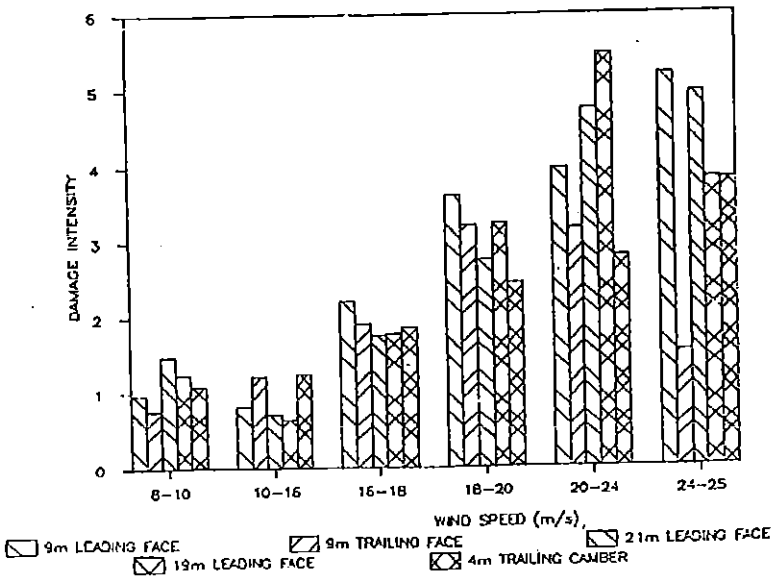

Fig. 8 Fatigue damage intensity at different modes of operation calculated at five rotor radii

Concluding Comments

1. Fatigue life of the 60m diameter welded rotor steel of the LS1 wind turbine has been estimated using extensive monitoring data. The assessment of the fatigue damage was carried out using both, (a) life to crack initiation employing S-N curve and Miner's summation rule and, (b) by assuming crack propagation from initial defect and fracture mechanics procedure. The long term damage was predicted by considering the annual wind distribution at the site.

2. Using fracture mechanics analysis, the rate of the crack propagation, and hence the estimated life, was sensitive to the initial assumptions of defect size, threshold values and residual stresses. The analysis predicted that once a crack initiates, under extreme circumstances the propagation stage could be shorter then originally anticipated and therefore regular inspection of the rotor welded joints is recommended.

3. The estimates of fatigue lives that were based (a), on six months data from on-line continuos rainflow counting of cycles and (b), on the fatigue analysis based on series of 10 minutes time histories, predicted similar lives to initiation of cracks. This was irrespective of the measured location on the rotor.

4. Damage intensity, defined as the ratio between fatigue damage and the proportion of time of operation at a particular wind band, increased with increasing wind speed and with increased distance from the rotor center.

References

(1) KOEPPL G. W., (1982), Putnam's power from the wind - 2nd edition, Van Nostrand Reinhold Company, New York.

(2) SUTHERLAND H. J., VEERS P. S. and ASHWILL T. D., (1994), Fatigue life prediction for wind turbines: A case study on loading spectra and parameter sensitivity, ASTM STP 1250, Case studies for fatigue education, pp. 174-207.

(3) GARRAD A. D., (1990), Chapter 5: Forces and dynamics of horizontal axis wind turbines, in Wind Energy Conversion Systems, Edited by Freris L L, , Prentice-Hall International Editions,.

(4) BISHOP N. W. M. and SHERRAT F., (1990), A theoretical solution for the estimation of 'rainflow' ranges from power spectral density data, Fatigue & Fracture of Engnrg. Mater. struct., Vol 13, No 4, pp 311-326.

(5) BISHOP N. W. M., HU Z. and WANG R., (1993), Methods for the rapid evaluation of fatigue damage on the Howden HWP330 wind turbine, Proceedings BWEA 15 Conference, York, pp 261-267.

(6) FINGER R. W., (1980), Prediction model for fatigue crack growth in windmill structures, ASTM STP 714, pp 185-204.

(7) FINGER R. W., (1985), Methodology for fatigue analysis of wind turbines, Windpower 85, Proceeding of the AWEA Conference, pp 52-56.

(8) LINDLEY D. L., SIMPSON P. B., PROSSER E. R. and WALKER D. E., (1986), Construction of the LS1 3MW Wind Turbine, EWEC '86, Rome.

(9) SIMPSON P. B., LINDLEY D., LEE A. S. and CAESARI A. H., (1983), The 3MW Orkney Wind Turbine, 5th BWEA Conference, Cambridge,.

(10) WARREN J. G., WHITE C. and SIMPSON P. B., (1990), LS1 Performance, EWEA Conference, Madrid, Spain, pp 501-505.

(11) TWIDELL J. W., GAULD R., FERN D. and BURTON A., (1995), Recommissioning and operating the LS1 3MW, Burgar Hill, Orkney Wind Turbine, using novel crack repair, 5th BWEA Conference.

(12) DOWNING S. D. and SOCIE D. F. (1982), Simple rainflow counting algorithms, Int. J. Fatigue, Vol 4, No 1, pp 31-40.

(13) BRITISH AEROSPACE TECHNICAL NOTES, (1989), Private communication,.

(14) BRITISH STANDARD 5400: Part 10: 1980, "Steel, Concrete and Composite Bridges, Code of practice for fatigue".

(15) DOWLING E. D., (1993), Mechanical behaviour of material, Prentice-Hall International Editions.

(16) nCode Theoretical manual, (1990), nCode International Ltd, Sheffield, England,.

(17) ESDU Item 81011, (1985), Stress and Strength, Vol. 7.

Acknowledgements

The authors would like to thank the Wind Energy Group and the Department of Energy, UK, (contract ETSU/DTI/DOE W/24/00137/00/00) for their kind permission to use the monitoring data and to Dr John Warren for his significant contribution to this investigation.